

Measurement of the lifetime of excited-state electron bubbles in superfluid helium

Ambarish Ghosh* and Humphrey J. Maris

Department of Physics, Brown University, Providence, Rhode Island 02912, USA

(Received 4 January 2005; published 12 August 2005)

We report on the measurement of the lifetime of bubbles in superfluid helium that contain an electron in the $1P$ state. The $1P$ bubbles are produced by laser excitation of ground-state bubbles, and are detected by ultrasonic cavitation. Our measurements show that the lifetime of these excited bubbles is much less than the calculated lifetime for radiative decay and, hence, is determined by a nonradiative mechanism.

DOI: [10.1103/PhysRevB.72.054512](https://doi.org/10.1103/PhysRevB.72.054512)

PACS number(s): 67.40.Hf, 43.35.+d

I. INTRODUCTION

Electrons injected into liquid helium open up a cavity in the liquid from which helium atoms are excluded.¹ These so-called electron bubbles have been studied in many experiments, principally through measurements of their mobility. An electron bubble in superfluid helium is an interesting quantum-mechanical system.²⁻⁸ The size and shape of the bubble are influenced by the quantum-mechanical state of the electron, whereas the wave function and energy of the electron are, in turn, determined by the geometry of the bubble. When illuminated by light of the appropriate wavelength, the ground-state spherical ($1S$) bubble can be excited to different electronic energy states. The higher energy states can relax back to the ground state by emission of a photon or possibly by a nonradiative process. For radiative decay, the lifetime is given by the expression⁸

$$\tau = \frac{3\hbar c^3}{4e^2\omega^3} \frac{1}{|\langle 1P|z|1S \rangle|^2}, \quad (1)$$

where ω is the frequency of the emitted photon, and $\langle 1P|z|1S \rangle$ is the matrix element of the z coordinate of the electron between the $1S$ and $1P$ states that has azimuthal quantum number zero. The radiative lifetime of the $1P$ bubble has been calculated⁸ and is found to be $44 \mu\text{s}$ at zero applied pressure, increasing to $71 \mu\text{s}$ at -1.6 bar and to $48 \mu\text{s}$ at 2 bar. As far as we are aware, there has been no estimate of the nonradiative lifetime. In this paper, we report on a measurement of the lifetime of the $1P$ state.

II. EXPERIMENT

The idea of the experiment is as follows. Electrons are introduced into superfluid helium either by applying a large negative voltage to a sharp tungsten tip or from a β source immersed in the liquid. A CO_2 laser is used to excite electrons to the $1P$ state.⁹ These bubbles are detected using an ultrasonic method.¹⁰ If a sound wave propagates through the liquid and the negative pressure swing is sufficiently large, an electron bubble becomes unstable and begins to grow rapidly. The negative pressure that is needed to explode a bubble containing an electron in an excited state is smaller in magnitude than the pressure needed for a bubble in the ground state.⁹ As a result, it is possible to determine the fraction of electrons that are in the excited state through a

measurement of the probability of cavitation as a function of the sound amplitude. Although the experiment is straightforward, in principle, the determination of the lifetime from the quantities that are directly measured in the experiment is complicated, relies on a number of assumptions, and requires a numerical simulation.

Experiments were conducted in a stainless-steel cell that was thermally connected to the pot of a recirculating He^3 system. High-purity He^4 gas (99.999%) from a pressurized cylinder was cleaned by passage through a 77 K cold trap and then condensed into the cell. The temperature of the cell was measured by a calibrated Ge resistance thermometer and controlled by a metal film resistor heater. The cell was mounted in an optical Dewar that had metal heat shields at liquid-nitrogen and liquid-helium temperatures. Windows in the heat shields and the outer vacuum can provide optical access to the cell along paths that did not pass through the liquid nitrogen or helium. Although some radiation from room temperature with wavelength in the range that can excite electrons from the $1S$ to the $1P$ state is admitted into the cell, the intensity of this radiation is negligible compared to the intensity provided by the CO_2 laser.

The experimental cell contained a hemispherical piezoelectric transducer (PZT) of outer diameter 2 cm, a metal ring, and a tungsten tip, as shown in Fig. 1(a). The tip was made by electrochemically etching a tungsten wire in a 10% NaOH solution. The tip had a typical threshold voltage for field emission between -500 and -1000 V. The current to the ring was typically around 1 nA. The ring was placed between the tip and transducer, and was connected through a $10^{11} \Omega$ resistor to an electrometer. This resistor served to stabilize the current through the tip. The ring had an inner diameter of 0.5 cm, an outer diameter of 1.5 cm and was 0.1 cm thick. A significant fraction of the electrons coming from the tip went into the ring. The fraction that entered the region below the transducer could be adjusted by applying a dc voltage to the lower face of the transducer. Thus, the ring made it possible to operate the tip with a voltage bias that results in a stable emission current while at the same time achieving the desired electron density in the region below the transducer.

In some of the measurements [see Fig. 1(b)], we used a Ni-63 β source to introduce electrons into the liquid. The source was a foil ($1.3 \text{ cm} \times 0.9 \text{ cm} \times 0.005 \text{ cm}$ thick) clamped between two brass disks. The upper disks had an aperture, $1.3 \text{ cm} \times 0.7 \text{ cm}$, through which electrons entered

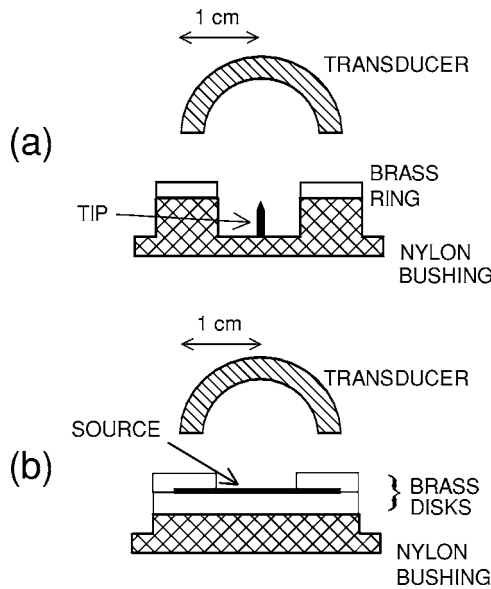


FIG. 1. Schematic diagram of the experimental setups that used (a) a tungsten tip and (b) a radioactive source to inject electrons into the helium.

the liquid. The effective activity of the source was 5 mCi. The disks had an outer diameter of 1.5 cm and were 0.13 cm thick. The disk-source system was placed about 0.5 cm below the focus of the transducer. The voltage to the disks could be altered to give the desired electron density in the region between the transducer and the source. Usually, the peak density of electrons was achieved by applying a small negative voltage (≈ -15 V) to the source.

Injection by means of the tip has the advantage that the number of electrons in the liquid can be controlled externally during the experiment. In addition, a higher electron density can be achieved than is possible with the radioactive source. However, as discussed later, the tip has the disadvantage that, in addition to 1S bubbles, it introduces a small number of other objects of unknown structure.

The light from the CO_2 laser¹¹ that was used to excite the electron bubbles passed through a ZnSe window on the outer can and through apertures on the 77 and 4 K heat shields. The aperture on the 77 K shield was $0.3 \text{ cm} \times 0.5 \text{ cm}$, the small size being chosen to minimize the amount of room temperature radiation entering the cell. The light entered the cell through a ZnSe window and, after passage across the cell, was absorbed by the sapphire window on the opposite side. The optical reflectivity of the sapphire at $10.6 \mu\text{m}$ (wavelength of the CO_2 laser) was measured to be $<1\%$. Light pulses of duration $400 \mu\text{s}$ were applied. The timing of these pulses was arranged so that the pulse began $350 \mu\text{s}$ before the arrival of the sound pulse at the acoustic focus. In estimating the intensity of the CO_2 laser light at the acoustic focus, it was necessary to allow for the divergence of the laser beam and for the losses due to reflection at the two uncoated ZnSe windows that the light passed through before entering the cell. The width of the light beam at the acoustic focus was several millimeters, and hence the intensity varied by only a very small amount over the region of the acoustic focus. The size of the focal region is approximately one half of the sound wavelength λ ($\lambda = 180 \mu\text{m}$).

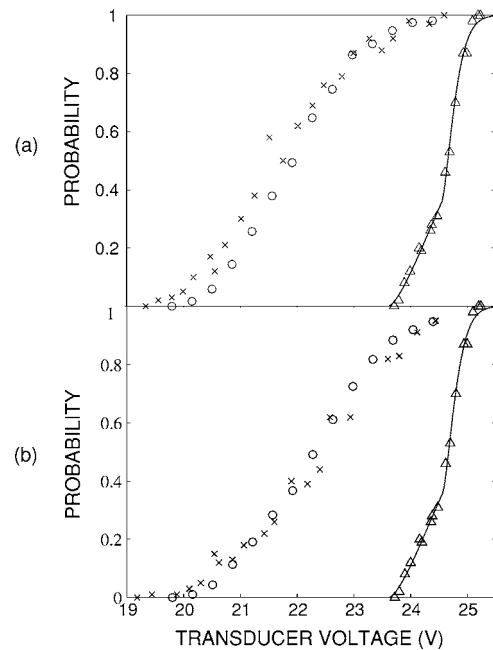


FIG. 2. Measurements of the probability of cavitation as a function of the voltage applied to the ultrasonic transducer. The triangles in both the figures are data taken without CO_2 illumination. The crosses are results when the intensity of the CO_2 illumination was (a) 61 W cm^{-2} and (b) 42 W cm^{-2} . The solid curve and the circles are the results of the simulation described in the text. The sound frequency was 1.35 MHz, the transducer was driven for 14 cycles, the temperature was 1.9 K, and the liquid helium in the cell was at the saturated vapor pressure. Electrons were injected into the cell using the tungsten tip.

For most measurements, we drove the transducer at its fundamental thickness mode frequency of 1.35 MHz with an rf pulse of duration 14 cycles. The rf pulses applied to the transducer had a repetition rate of 1/s. The peak-to-peak voltage V_{tran} of the last cycle of oscillation on the transducer was measured using a digital oscilloscope. The typical standard deviation in the voltage measurement was $<0.4\%$. The pressure oscillation in the acoustic focus was assumed to be proportional to V_{tran} . Usually around 200 pulses of voltage V_{tran} were sent to the transducer. The ratio of the number of explosion events to the number of applied voltage pulses gave us the probability S of explosion. The cavitation bubbles were detected using light from a He-Ne laser that was focused into the region of the acoustic focus. When a bubble exploded, light that was scattered by a small angle was detected by a photomultiplier. The He-Ne laser light entered and left the cell through Al_2O_3 windows on the outer can, fused silica windows on the 77 and 4 K shields, and Al_2O_3 windows on opposite sides of the cell.

Experimental data taken under different experimental conditions along with the results of numerical simulations to be described in Sec. III are shown in Figs. 2–5. Figure 2 shows the results obtained with liquid helium at 1.9 K under the saturated vapor pressure (SVP) and driving the transducer at its fundamental frequency of 1.35 MHz. By exciting the third harmonic of the transducer, we also made a measurement at 4.25 MHz at SVP. Results are shown in Fig. 3.

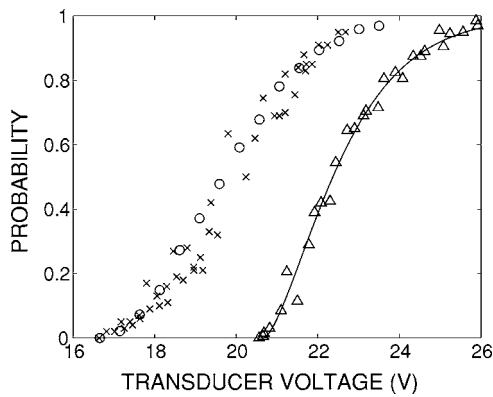


FIG. 3. Measurements of the probability of cavitation as a function of the voltage applied to the ultrasonic transducer. The experimental conditions were the same as in Fig. 2 except that the frequency of the sound was 4.25 MHz and the transducer was driven for 20 cycles.

Measurements at this frequency are more difficult because after cavitation occurs, the bubbles do not grow to as large a size as they do at 1.35 MHz, and hence are harder to detect. Figure 4 shows measurements made at 1.35 MHz with a static pressure in the cell of 0.83 bar. In Fig. 5 we show data taken at 1.4 K and SVP using the radioactive source to inject electrons.

III. NUMERICAL SIMULATIONS

Consider first the situation when there is no CO_2 illumination so all electron bubbles should be in the $1S$ state. In this case cavitation first begins to occur when the negative pressure at the focus reaches a critical pressure of P_{1S}^c . Above the voltage needed to produce this pressure, the probability of cavitation should increase rapidly as the applied voltage is raised because the region around the focus in which the pressure swings below P_{1S}^c becomes larger. There is then a greater chance of an electron bubble being contained within this volume. The rate at which the probability

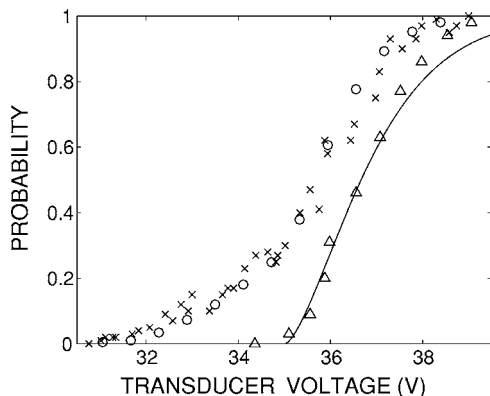


FIG. 4. Measurements of the probability of cavitation as a function of the voltage applied to the ultrasonic transducer. The experimental conditions were the same as in Fig. 2, except that the CO_2 intensity was 42 Wcm^{-2} , the pressure was 0.83 bar, and the electrons were injected into the cell using the radioactive source.

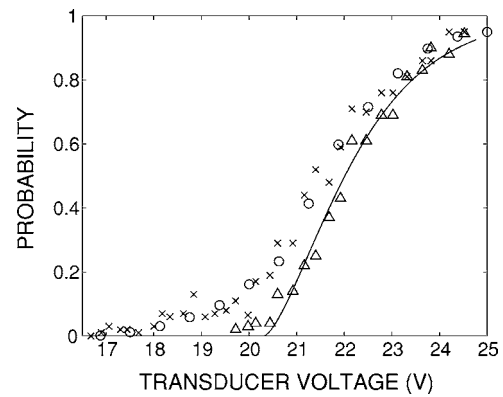


FIG. 5. Measurements of the probability of cavitation as a function of the voltage applied to the ultrasonic transducer. The experimental conditions were the same as in Fig. 2, except that the CO_2 intensity was 61 Wcm^{-2} , the temperature was 1.4 K, and the electrons were injected into the cell using the radioactive source.

increases will be more rapid if the number density of the electrons is large. Consider now the data in Fig. 2. It can be seen that there is no cavitation when the transducer voltage is below 23.7 V. The probability then rises slowly up to a voltage of around 24.6 V and then begins to rise much more rapidly and quickly becomes close to unity. We believe that the rapid rise in the range above 24.6 V is due to $1S$ electron bubbles and that the slow rise in the probability below this voltage is due to some other objects $1\tilde{S}$ of much lower density. It is possible that these other objects are electron bubbles that are attached to quantized vortices, but we have not been able to prove this. The $1\tilde{S}$ bubbles are only seen when electrons are injected using the tip and have not been detected when the radioactive source was used.

To estimate the number of normal $1S$ bubbles and $1\tilde{S}$ bubbles, we proceeded as follows. We first estimated the spatial variation of the sound field around the focus. Let the peak-to-peak voltage driving the transducer be V_{tran} and let τ_{tran} be the time that it takes for the vibration of the transducer to damp out when it is not driven. When the transducer is driven at resonance, its oscillation amplitude $A(t)$ at time t builds up according to the relation

$$A(t) = CV_{\text{tran}}[1 - \exp(-t/\tau_{\text{tran}})], \quad (2)$$

where C is a constant. To determine τ_{tran} , we drove the transducer for a long time at some fixed amplitude and then recorded the voltage appearing on the transducer as a function of the time after the drive was turned off. The results for τ_{tran} were 5.4 and 2.2 μs for the 1.35 and 4.25 MHz modes, respectively. These damping times correspond to Q values of 23 and 30 at the two frequencies. To calculate the pressure field in the vicinity of the acoustic focus,¹³ we used the method described by O'Neil.¹² In this approach, the sound amplitude at any point \vec{r} in the liquid is calculated by adding up contributions propagating to \vec{r} from each point on the surface of the transducer. Then allowing for the variation of the transducer amplitude with time as given by Eq. (2), we obtain an estimate for the pressure in the vicinity of the

acoustic focus¹³ as a function of \vec{r} and t . The experimental data gives the value of the threshold transducer voltage V_{tran}^{1S} (24.6 V) at which the pressure swing at the focus first becomes large enough to cause 1S bubbles to explode. To determine the value of P_{1S}^c at 1.9 K, we made measurements of how V_{tran}^{1S} varied with the static pressure in the cell. Assuming that the pressure swing at the focus is proportional to the transducer voltage, we can use these data to find P_{1S}^c and the value of the coefficient C appearing in Eq. (2). This then makes it possible to know the sound field in the vicinity of the acoustic focus as a function of time t , position \vec{r} , and transducer voltage. The value obtained for P_{1S}^c was -1.62 bar at 1.9 K. Similarly, the value for P_{1S}^c was obtained to be -1.85 bar at 1.4 K. These values are in good agreement with the earlier measurements of Classen *et al.*¹⁰

For any given voltage V_{tran} applied to the transducer, we can then calculate the total volume $v_{1S}(V_{\text{tran}})$ in the vicinity of the acoustic focus within which the pressure goes below the critical pressure P_{1S}^c at any time during the application of the sound pulse. For the $1\tilde{S}$ bubbles, the critical pressure is estimated as $P_{1S}^c \times (23.7/24.6) = -1.56$ bar. We then calculate the corresponding volume $v_{1\tilde{S}}(V_{\text{tran}})$ for these objects. We next make a trial guess at the number densities $n(1S)$ and $n(1\tilde{S})$ of the 1S and $1\tilde{S}$ objects. The probability that there are no 1S or $1\tilde{S}$ bubbles close enough to the acoustic focus to explode is then

$$\exp[-n(1S)v_{1S}(V_{\text{tran}}) - n(1\tilde{S})v_{1\tilde{S}}(V_{\text{tran}})]. \quad (3)$$

The probability that cavitation occurs for this applied voltage is then

$$1 - \exp[-n(1S)v_{1S}(V_{\text{tran}}) - n(1\tilde{S})v_{1\tilde{S}}(V_{\text{tran}})]. \quad (4)$$

The values of $n(1S)$ and $n(1\tilde{S})$ are then adjusted to give a best fit to the data as shown in Fig. 2. These fits gave $n(1S) = 2.7 \times 10^8 \text{ cm}^{-3}$ and $n(1\tilde{S}) = 2.3 \times 10^7 \text{ cm}^{-3}$. The same procedure was also used for the data (shown in Figs. 3–5). For the data shown in these figures, a good fit could be obtained without allowing for any contribution from $1\tilde{S}$ bubbles.

We now consider the analysis of the data in Fig. 2 that were taken in the presence of illumination. Let the cross section for the $1S \rightarrow 1P$ transition be σ , the light intensity I , and the $1P$ lifetime τ . Then the number density $n(1P)$ of $1P$ bubbles and the density $n(1S)$ of ground-state bubbles should vary with time as

$$\frac{\partial n(1P)}{\partial t} = \frac{I\sigma}{\hbar\omega} n(1S) - \frac{n(1P)}{\tau} \quad (5)$$

$$\frac{\partial n(1S)}{\partial t} = -\frac{I\sigma}{\hbar\omega} n(1S) + \frac{n(1P)}{\tau}, \quad (6)$$

where ω is the frequency of the incident photon. Note that there is no term in these equations arising from stimulated emission. This is because almost immediately after a bubble is excited to the $1P$ state, the shape and size of the bubble

changes.¹⁴ After this time the photon energy required to cause stimulated emission has shifted by a large amount and so the CO_2 radiation cannot enhance the rate at which $1P$ bubbles relax.

Under steady illumination the ratio of the number densities of excited- and ground-state bubbles is

$$\frac{n(1P)}{n(1S)} = \frac{I\sigma\tau}{\hbar\omega}. \quad (7)$$

When planning the experiment, we had assumed that the lifetime of the $1P$ bubbles might be limited by radiative decay and, therefore, we anticipated a lifetime of around $40 \mu\text{s}$. If this were the situation, the lifetime would be significantly greater than the duration of the sound pulse ($10.4 \mu\text{s}$ for the measurements at 1.35 MHz) and also considerably less than the length of time during which light was applied before the application of the sound. Consequently, under these conditions the ratio of $n(1P)$ to $n(1S)$ should be as given by Eq. (7). This equation predicts that the population of excited- and ground-state bubbles becomes equal for an intensity of

$$I_{1/2} = \frac{\hbar\omega}{\sigma\tau}. \quad (8)$$

For a cross section of the order of 10^{-15} cm^2 , a photon energy of 0.117 eV, and a lifetime of $40 \mu\text{s}$, the intensity $I_{1/2}$ is 0.5 W cm^{-2} . In preliminary experiments, we found that for an intensity in this range, only a small percentage of the bubbles were in the $1P$ state. This indicated that the actual lifetime is considerably less than the radiative lifetime.

The short lifetime considerably complicates the analysis of the experiment. The photon energy required to excite the 1S bubble to the $1P$ state depends on the pressure. Thus, during each cycle of the sound wave, the absorption cross section changes by a significant amount. This cross section is largest when the pressure is around 1 bar and is small when the pressure is negative. Consequently, in order for cavitation to result from the explosion of a $1P$ bubble, the bubble has to be excited when the pressure is positive and survive until the pressure has become large and negative. Because of this variation of the cross section with pressure it is necessary to perform a numerical simulation in order to analyze the experimental data.

As a first step, we calculated the $1S \rightarrow 1P$ cross section. The energy E_{1S-1P} to excite from the 1S to the $1P$ state has been measured by Grimes and Adams¹⁵ as function of pressure for positive pressures at 1.3 K. Grimes and Adams, also Maris,⁸ have calculated E_{1S-1P} on the basis of a simplified model and obtained good agreement with the experimental data. The calculation of Maris also predicts the variation of E_{1S-1P} in the negative pressure regime. We have modified this calculation slightly to allow for the small difference in the surface tension between the temperature of the Grimes and Adams experiment (1.3 K) and the temperatures at which the measurements of the present experiment (1.9 and 1.4 K) were obtained. The result for E_{1S-1P} is shown in Fig. 6. Recently, Maris and Guo¹⁶ have calculated the line shape for the $1S \rightarrow 1P$ transition, taking into account the effect of zero-point and thermal fluctuations on the shape of the elec-

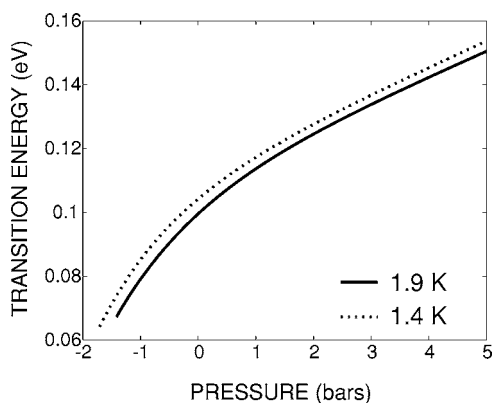


FIG. 6. Calculated photon energy E_{1S-1P} required to excite the $1S$ to $1P$ transition as a function of pressure at 1.9 K (solid line) and 1.4 K (dotted line).

tron bubbles. The calculated line shape at 1.3 K was in excellent agreement with the experimental results of Grimes and Adams. We used the same method together with the estimate for E_{1S-1P} to obtain the absorption cross section for the CO_2 laser energy of 0.117 eV as a function of pressure at 1.9 and 1.4 K. The results are shown in Fig. 7.

We then used these results to perform a computer simulation to compare to the measured cavitation probability in the presence of illumination. For the total density n of electron bubbles per unit volume [$n=n(1S)+n(1P)$], we use the value of $n(1S)$ measured in the absence of CO_2 laser radiation.¹⁷ We assume trial values for the $1P$ lifetime τ . We then place electron bubbles at random positions in the vicinity of the acoustic focus with a density n . For each bubble in turn, we then simulate the effect of the applied CO_2 laser radiation. We start the simulation at the time that sound first arrives at the focus ($t=0$). At this time, each bubble is randomly assigned to be either in the $1S$ or the $1P$ state with probability consistent with the equilibrium distribution given by Eq. (7). We choose a simulation time step of $\delta t=10^{-9}$ s. At each time step there is a probability P_{1S-1P} of the bubble making a transition to the $1P$ state, given by

$$P_{1S-1P} = \frac{I\sigma}{\hbar\omega} \delta t. \quad (9)$$

The probability of return from $1P$ to $1S$ per unit time is $P_{1P-1S} = \delta t/\tau$. At each time interval, we use in Eq. (9) the cross section σ calculated for the instantaneous value of the pressure at the position of the bubble. We continue the simulation until the pressure oscillations have decayed to the point that the negative pressure swing does not become more negative than P_{1P}^c . If at any time, the bubble is in the $1P$ state and $P < P_{1P}^c$, or the bubble is in the $1S$ state and $P < P_{1S}^c$, then the bubble will explode. In this case, the result of the simulation is that cavitation occurs and we then move on to simulate another random distribution of electrons. If the bubble does not explode, we proceed to perform a simulation for the other bubbles. If none of the bubbles explode, then cavitation does not occur.

Note that we do not make any allowance for the motion of the bubbles. Under the influence of the electric field in the part of the experimental cell near to the acoustic focus, the bubbles move with drift velocity typically of the order of 1 cm/s. Hence, the distance they travel in the time that the sound wave is applied is very small compared to the acoustic wavelength.

The simulation is repeated for 2000 different random distributions of electrons, and from the results we obtain the probability of cavitation. This is then repeated for a series of values of the transducer voltage to create a plot of the simulated cavitation probability S_{sim} as a function of V_{tran} . Finally, the value of τ and P_{1P}^c are adjusted so that the results of the simulation are in best possible agreement with experiment. The best agreement with experiment was with $P_{1P}^c = -1.30$ bar at 1.9 K and $P_{1P}^c = -1.48$ bar at 1.4 K. The values of τ that gave the best fit with experiment for the two intensities shown in Fig. 2 were 55 and 53 ns, respectively.

We then made a similar analysis for the data taken at static pressure 0.83 bar (shown in Fig. 4) and obtained a best fit for 50 ns. Note that for the data shown in this figure the radioactive source was used and so there was no possible complication arising from $1\tilde{S}$ bubbles. For the data at 4.25 MHz (see Fig. 3), the best fit for τ was 45 ns. Note that at this frequency the acoustic wavelength is three times smaller and so the effective volume of the acoustic focus is 27 times smaller. As a result, for a given electron density the probability of cavitation is smaller by a factor of 27 and the contribution from the $1\tilde{S}$ bubbles cannot be clearly seen. Analysis of the data taken at 1.4 K (shown in Fig. 5) gives a lifetime of 48 ns.

Because the lifetime is determined by comparison of the data to the result of a complex numerical simulation, it is hard to make a serious estimate of the uncertainty. The lifetime as determined from the data shown in Figs. 2–5 was found to have the values 55, 53, 50, 45, and 48 ns, respectively, giving an average value of 50 ns with a rms fluctuation of 4 ns. However, we recognize that there may be some unknown source of systematic error that affects τ as determined from each data set in approximately the same way.

IV. DISCUSSION

The agreement between the values of τ obtained from the different measurements is very encouraging. The agreement

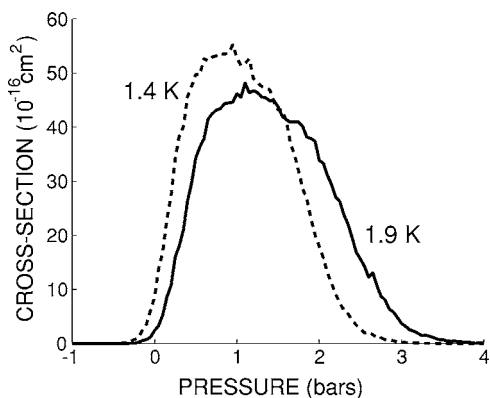


FIG. 7. Calculated cross section for the $1S$ to $1P$ transition for photons of energy 0.1167 eV as a function of pressure at 1.9 K (solid line) and 1.4 K (dashed line).

between the results obtained at 1.9 and 1.4 K suggests that the lifetime is independent of temperature. It would have been interesting to make measurements down to lower temperatures, but it is difficult to obtain a high density of electron bubbles at low temperatures because the mobility increases rapidly as the temperature is lowered.¹⁸

We have implicitly assumed in making the simulations that the lifetime τ can be treated as approximately constant over the pressure range from around 1 bar, the pressure at which light is absorbed, to the explosion pressure. To some limited extent this assumption is supported by the fact that measurements at different frequencies and ambient pressures give the same values for τ . Possibly a better test of the assumption that τ is constant could be made by using a different wavelength to excite the bubbles so that the maximum absorption would occur at a different pressure.

We are unaware of any calculation of the nonradiative lifetime for electron bubbles in helium, although there is extensive literature regarding the nonradiative decay of excited states of impurity atoms and ions in classical liquids.¹⁹ The

key question is how does the electron energy get transferred to the degrees of freedom of the liquid. The energy that the $1P$ state has to lose to return to the $1S$ state is estimated to be 0.04 eV or 460 K.²⁰ This is sufficient to create more than 50 rotons, and we do not know how to calculate quantitatively the relaxation rate for such a high-order process. Alternatively, one could perhaps consider the transfer of the energy from the electron to one or more atoms on the surface of the bubble or to one of the vibrational modes of the bubble surface.

ACKNOWLEDGMENTS

We thank D.O. Edwards and R.M. Stratt for helpful discussions and W. Guo for providing the computer program that was used in the calculation of the absorption cross section of the electron bubbles. This work was supported, in part, by the National Science Foundation through Grant No. DMR-0305115.

*Present address: Rowland Institute at Harvard, 100 Edwin H. Land Blvd., Cambridge, MA 02142. Electronic address: ghosh@rowland.harvard.edu

¹For a review of early work on this subject, see A. L. Fetter, in *The Physics of Liquid and Solid Helium*, edited by K. H. Benneman, and J. B. Ketterson (Wiley, New York, 1976), Chap. 3.

²E. P. Gross and H. Tung-Li, *Phys. Rev.* **170**, 190 (1968).

³W. B. Fowler and D. L. Dexter, *Phys. Rev.* **176**, 337 (1968).

⁴B. DuVall and V. Celli, *Phys. Lett.* **26A**, 524 (1968); *Phys. Rev.* **180**, 276 (1969).

⁵D. L. Dexter and W. B. Fowler, *Phys. Rev.* **183**, 307 (1969).

⁶H. J. Maris, *J. Low Temp. Phys.* **120**, 173 (2000).

⁷T. Miyakawa and D. L. Dexter, *Phys. Rev. A* **A1**, 513 (1970).

⁸H. J. Maris, *J. Low Temp. Phys.* **132**, 77 (2003).

⁹D. Konstantinov and H. J. Maris, *Phys. Rev. Lett.* **90**, 025302 (2003).

¹⁰J. Classen, C.-K. Su, M. Mohazzab, and H. J. Maris, *Phys. Rev. B* **57**, 3000 (1998).

¹¹Synrad Inc., Mukilteo, Washington, Model J48-1.

¹²H. T. O'Neil, *J. Acoust. Soc. Am.* **21**, 516 (1949).

¹³Note that by the term "focus" we are referring to the point in the liquid at which the pressure oscillation has the largest amplitude. For a hemispherical transducer this point is not precisely at the center of curvature.

¹⁴These changes occur in a timescale of the order of 10^{-11} s.

¹⁵C. C. Grimes and G. Adams, *Phys. Rev. B* **41**, 6366 (1990); **45**, 2305 (1992).

¹⁶H. J. Maris and W. Guo, *J. Low Temp. Phys.* **137**, 491 (2004).

¹⁷Note that it is not clear how to treat the unidentified $1\bar{S}$ objects. However, these only amount to 7% of the total number of bubbles so we have ignored any contribution to the cavitation probability arising from them.

¹⁸In the experiment of Classen *et al.* (Ref. 10), a high density was achieved at temperatures below 1 K by applying a large enough electric field so that the bubbles became trapped on vortices.

¹⁹See, for example, D. W. Oxtoby, *Adv. Chem. Phys.* **47**(P2), 487 (1981); J. C. Owrutsky, D. Raftery, and R. M. Hochstrasser, *Annu. Rev. Phys. Chem.* **45**, 519 (1994).

²⁰This is the value for $P=0$ as calculated in Ref. 8.